Available online at www.sciencedirect.com

ScienceDirect

Procedia Engineering 110 (2015) 128 – 134

Procedia Engineering

www.elsevier.com/locate/procedia

4th International Conference on Tissue Engineering, ICTE2015

Hybrid fabrication of a 3D printed geometry embedded with PCL nanofibers for tissue engineering applications

Christian Mendoza-Buenrostro[a,*], Hernan Lara[a], Ciro Rodriguez[a]

[a]*Centro de Innovación en Diseño y Tecnología, Tecnológico de Monterrey - Campus Monterrey, Av. Eugenio Garza Sada 2501, Monterrey 64849, México*

Abstract

A machine tool for the automatic fabrication of biocompatible scaffolds with embedded nanofibers mats was built. In this novel process, the scaffolds produced by Fused Deposition Modeling (FDM) were embedded with polycaprolactone (PCL) nanofibers in between the object layers. The nanofibers mat was obtained by far field electrospinning and its pore size was controlled by the fabrication process. An additional micromachining tool was used to drill and create microchannels in the hybrid geometry as required. This geometry will further be used in combination with cell cultures to study stem cell adhesion, proliferation and differentiation.

Peer-review under responsibility of IDMEC-IST

Keywords: Scaffolds; nanofibers; 3D printing; fused deposition modeling; electrospinning; cell cultures

1. Introduction

The field of tissue engineering and regenerative medicine have generated a vast amount of attention in the last years due to their recognized potential in clinical areas. Traditionally, cell cultures are grown on two-dimensional (2D) containers such as Petri dishes, and culture flasks. These allow the study of cellular behavior in a controlled laboratory environment. However, most of the cells inside the body are not constrained to a simple 2D substrate but to an intricate 3D design of extra cellular matrix (ECM). The ECM is composed of several molecules segregated by the surrounding cells. Some of the ECM basic functions are to allow cell adhesion, cell-to-cell communication, and cell differentiation

* Corresponding author. Tel.: +52-81-8288-1879.
E-mail address: christian.mendoza@itesm.mx

Peer-review under responsibility of IDMEC-IST
doi:10.1016/j.proeng.2015.07.020

[1]. Cells grown on traditional 2D containers may not be reacting in the same way as their *in vivo* counterparts because of the lack of appropriate ECM signals such as physical or biochemical cues. Furthermore, the ECM characteristics differ from one type of tissue to another (i.e. osteoblasts ECM differs greatly from neuronal cells ECM, their respective ECM Young Modulus are very different). Additionally, it has been shown that the topology and chemistry of the ECM affects stem cells differentiation towards one or another type of cell lineage [2-4]. Therefore, it is of great interest to develop materials and techniques that allow for the manufacturing of 3D scaffolds that could better resemble the ECM to which cells are exposed in a natural *in vivo* environment.

Some of the aspects to consider when building such 3D scaffolds for cell culture attachment and growth are mechanical stability, porosity, surface chemistry, topography, pore interconnectivity, and biocompatibility. Several techniques for scaffold fabrication have been explored, such as electrospinning which has been extensively used to create scaffolds for tissue engineering [5-7]. Other fabrication techniques such as Solid Free Form (i.e. laser, droplet and nozzle based techniques) have recently been exploited for tissue engineering and regenerative medicine [8-10]. However, due to the complexity of the different types of ECM, no single fabrication technique suffices to obtain a fully detailed 3D scaffold, closely resembling a naturally occurring ECM. Therefore, it is needed a combination of fabrication techniques that integrates biocompatible materials and manufacturing in scales of millimeters to micrometers to fabricate 3D scaffolds for tissue engineering applications.

In this work, it is presented a machine design to allow for the fabrication of biodegradable hybrid 3D scaffolds using a combination of three different manufacturing techniques such as FDM, electrospinning, and micromilling. Electrospun fiber mats are embedded in between the FDM fabricated layers to create a 3D scaffold environment, with a topography having a scale range from millimeters to nanometers. The micromilling process provides for development of additional structure features such as microchannels to the scaffold.

2. Materials and methods

2.1. Extruder

The extruder was obtained from the RapMan v3.1 FDM printer (Bits from Bytes). The extruder is composed of a heater element (Ni-chrome wire), a high heat-resistance and high sensitive thermistor (504GT thermistor), a stepper motor, and a holding structure. The thermistor has a sensing range from -50 ºC to 300 ºC. The extruder maximum working temperature is 280 ºC. This extruder uses a 3 mm PLA filament also obtained from Bits from Bytes. The extrusion temperature was set to 190 ºC.

2.2. Micromilling machine

The micromilling machine in this work, NSK Nakanishi EM-3060 Brushless Motor, was placed in a vertical position. Its motor speed range is 1000 rpm to 60,000 rpm. The tool to test the device was a SGS-39240-MK2M general purpose microsquare nose end mill (carbide material, 1.02 mm cutting diameter).

2.3. Electrospinning

The high voltage power supply for electrospinning is a Gamma High Voltage Research, ES20P-5W. The experiments were run using a voltage set to 17 kV for each experiment. An aluminium squared collector of 10 x 10 cm was set as the ground electrode for electrospinning. As an option, copper stripes in an “L” shape were chosen as ground electrode. A blunt needle (18G) was set as the working electrode. The distance between needle and ground collector was set to 15 cm for the experiments.

2.4. Polymer solution

The polymer solution was prepared from PCL and acetone as solvent in 10% wt. The PCL (MW 80,000) was bought from Sigma Aldrich and acetone was analytical grade. The polymer solution was stirred overnight at 30 ºC in a closed container to avoid evaporation. Once the solution was ready, a further filtering step was implemented to remove any PCL remnants in the polymer solution. Afterwards, the solution was brought to 20 ml syringes and stored for later use during the same day. A syringe pump, KDS-100 (KDS Scientific) perfused the polymer solution during electrospinning. The syringe pump was set to a flow rate of 2 to 4 ml/hr.

2.5. Programming code

A custom made program was developed and implement using Labview. The program allows for direct writing of G-code commands to control the movement of all the axes (5) of the device, as well as the control of the amount of time that electrospinning was left active, and the control of the micromilling spindle. It is also possible to import a premade text file with all the G-code commands to automatically control the functions of the device (i.e. extrusion, micromilling, and electrospinning).

2.6. Machine axes and electronics

One of the axis (LM Guide Actuator KR) (stroke length of 60 cm) was obtained from THK. A second axis (MS25, Thomson Linear Motion) has a stroke length of 25 cm. The first two axes described are assembled in an (x, y) manner. The vertical axes holding the tools are servomotors from National Aperture, MM-4M-F-50, 50 mm in stroke length, ±0.5 µm in repeatability, ±0.1 µm in precision. A MC-4SA driver from National Aperture powered the servo motors. Three other drivers from SPARKFUN (Easy Driver) provided power to the stepper motors of the rest of the linear guides (x and y direction, and extruder motor). Two Arduino Mega were implemented in the electronic design. One of the Arduino microcontroller was dedicated to the movement control of the x, and y axes, as well as the extruder stepper motor, while a second microcontroller was dedicated to control the temperature of the extruder filament. A dedicated PC running Labview and NI-PCI 7356 card completed the control system.

2.7. Machine assembly and operation

As starting point for this prototype concept, rapid prototyped printed parts were obtained (ABS). These parts were elaborated in a Fortus 400MC 3D printer. Figure 1a shows a CAD assembly for the tools, axes and supporting base, and figure 1b shows the assembled machine. In a further development, these ABS parts will be replaced with metallic components to increase the prototype rigidity and accuracy.

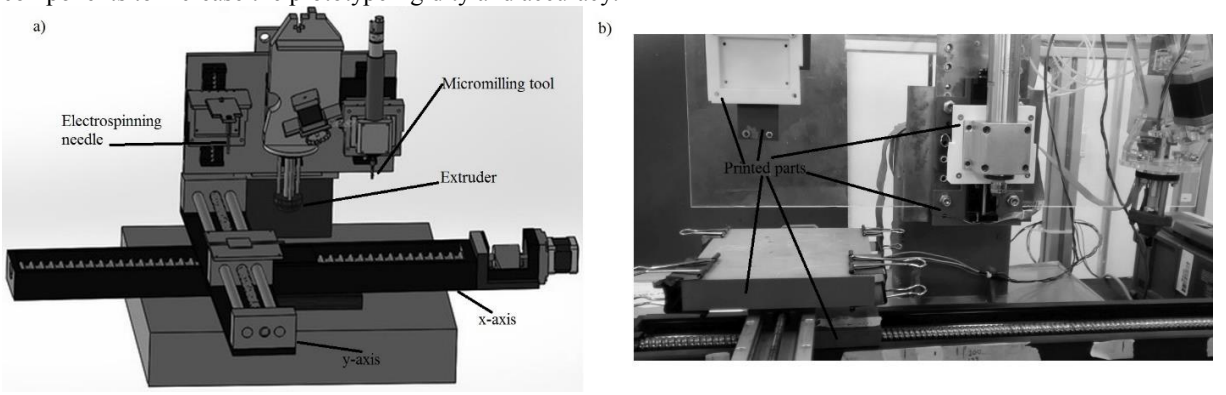

Fig. 1. (a) CAD design; (b) real life assembly.

The process for the fabrication of the hybrid 3D scaffolds is as follow. First, an extruded layer consisting of contiguous extruded stripes is placed on the printing bed, this will be the bottom layer. Next, a squared first layer is deposited on top of the bottom layer. Once the first squared layer is in place, the extrusion stops and the x axis moves the printing bed towards the electrospinning needle. After the stage is positioned below the needle, the x axis stops and electrospinning starts by turning on the power supply and syringe pump for a set amount of time. The amount of time that electrospinning process is activated is predefined during the initial setup. When the electrospinning process stops, the x axis returns to the last position at extrusion and continues fabricating the 3D scaffold. This process repeats as many times as there are layers to be fabricated. The amount of time that electrospinning process is active can be set to a different value in each of the 3D scaffold layers.

3. Results and discussion

A simple squared structure of 1 by 1 cm embedded with PCL fibers was manufactured as described in section 2.7 to confirm that the machine was able to produce the intended 3D scaffolds. Figure 2 shows a typical result for a 3D printed squared structure (PLA) embedded with PCL fibers. The structure in figure 2 has 13 layers in total, from which five of them were coated with electrospun fibers. The time spent during the electrospinning step in each layer was set to 3 min/layer and polymer flux of 3ml/hr. For each extruded layer, the layer height was defined as 100 µm. A full PLA layer was placed at the bottom of the extruded structure to provide with good adhesion to the printing bed. A finer inspection under microscope reveals the existence of fibers at different focal points.

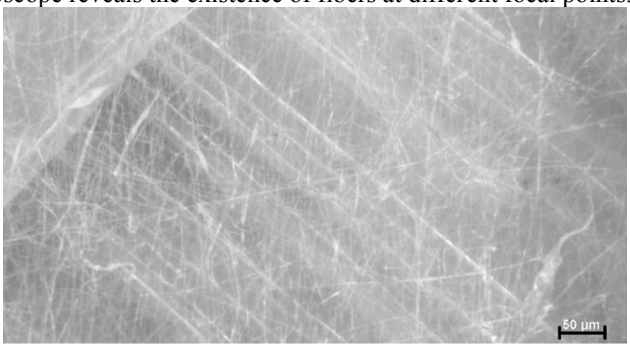

Fig. 2. 3D scaffold embedded with PCL fibers (top view).

In figure 3 it is shown typical fiber sizes obtained in the fiber mat. The electrospun fibers in this sample have an average diameter of 2.6 µm (std=0.44). It can be seen from figure 3 that there are electrospun fibers in different heights of the 3D structure, this is due to the different layers in which they were electrospun during the scaffold manufacturing.

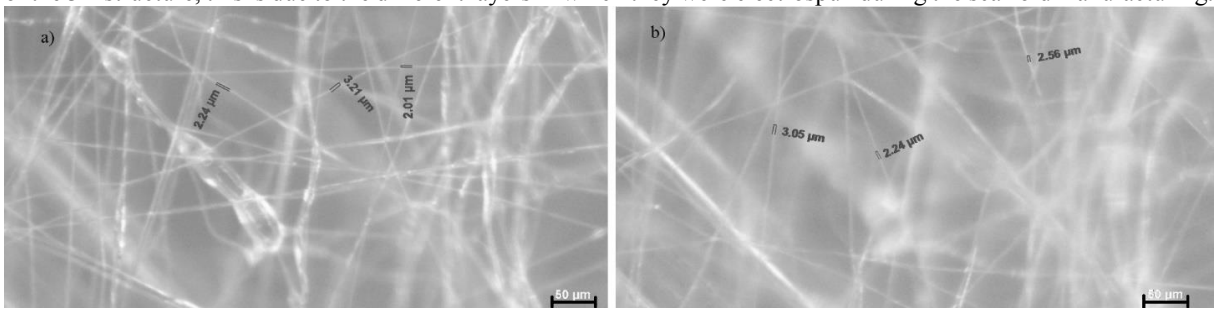

Fig. 3. (a) Typical fiber diameter; (b) same as (a) with different focus.

It is also important to consider the scaffold porosity and pore interconnectivity when fabricating scaffolds for tissue engineering applications. These two aspects provides for nutrient diffusion and cellular waste that occurs naturally during a cell culture. The porosity of the hybrid scaffolds was determined using ImageJ software. A porosity of 53.61% was obtained after 60 seconds of activating electrospinning during each of the five layers. Likewise, it was also possible to change the porosity of the scaffold by changing the amount of time that electrospinning was left active during each layer. For example, in another experiment, the porosity of the scaffold using the same structure and methodology from figures 2 and 3 was 42.91% after 3 minute of electrospinning being active during each of the 3D printed layers. This results indicates that the longer electrospinning is active, the less porous the scaffold will be. This could potentially influence the nutrient and cell diffusion throughout the hybrid scaffold layers. Future work will be carried out to characterize the hybrid scaffold porosity based on the electrospinning activation time per layer.

In order to test the basic function of the micromilling tool, several slot lines were elaborated on the PLA structure. Figure 4 shows an example for a straight slot line (Ra= 5.62 µm) using the micromilling tool were the rpm was set to 30,000 rpm, stage velocity of 960 mm/min, and depth of 0.5 mm. The linear actuator for the x-axis can reach a maximum speed of 1200 mm/min. However, recommended stage velocity for plastics is in the range of 156,000-234,000 mm/min, and 195,000-293,000 mm/min for slot and profile milling respectively. Therefore, the results shown in figure 4 are not ideal, PLA melts and small portions of it adheres to the micromilling tip. However, it was proven that the control system can actuate the micromilling tool and create basic features on the PLA structure. Future work will be carried out to modify the setup in order to improve the machine tool micromilling capacity.

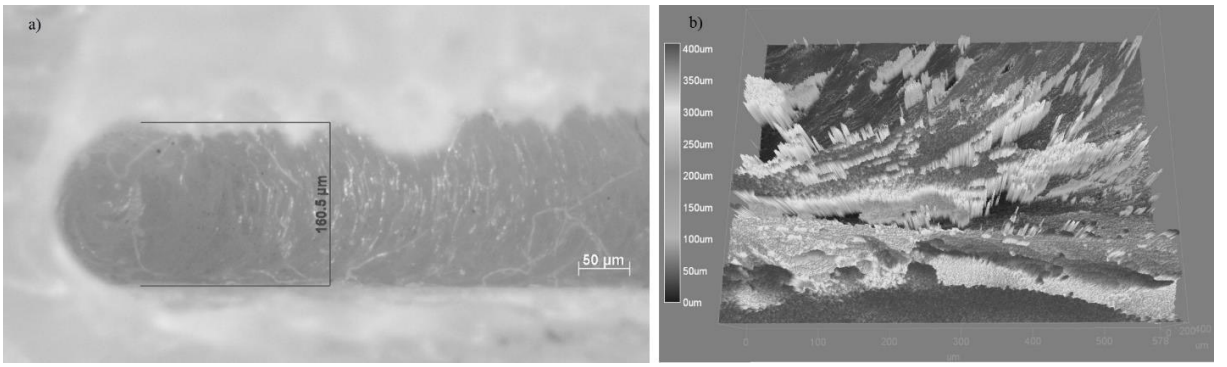

Fig. 4. (a) Micromilled slot line; (b) confocal 3D image for (a).

Another example of a hybrid scaffold structure is shown in figure 5, a Scanning Electron Microscope (SEM) image show the embedded fibers between the extruded polymer layers. The thicker supporting structure was extruded from ABS filament in this case, and the thinner fibers were electrospun from PCL polymer solution as described in section 2. It is observed that PCL fibers are located in different layers of the structure, this was corroborated by the different focus points needed to properly observe different areas of the suspended PCL fibers. Such hybrid structure can potentially provide cells with mechanical cues and anchor points to facilitate attachment, diffusion and help sustain proliferation and differentiation, eventually leading to a desired tissue. These first experimental results give an indication that it is possible to combine different materials in this process.

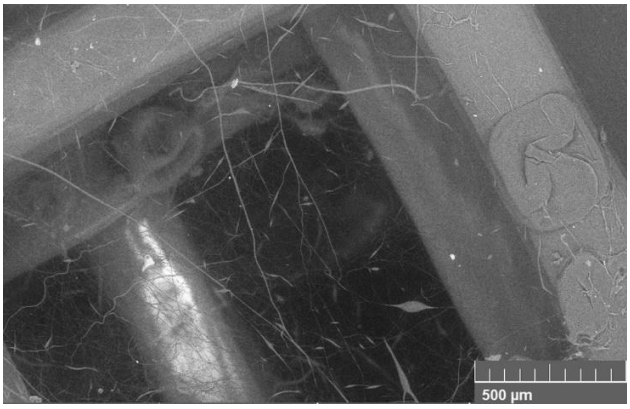

Fig. 5. Hybrid scaffold structure.

In figure 6 it is shown another example for the capabilities of combining FDM extrusion and electrospinning. The results from polymer electrospinning can range from pure fibers when the polymer concentration is high (~7% to 12% w/v) to pure beads when the polymer concentration is low (~ <4% w/v). However, there is a middle range between the two which has a characteristic beads-on-string effect as observed in figure 6, remnant material is deposited along with fibers in a bead like manner. This particular effect could be used to regulate even further the porosity and surface of the fiber mats between the scaffold layers, potentially providing cells with additional supporting structure.

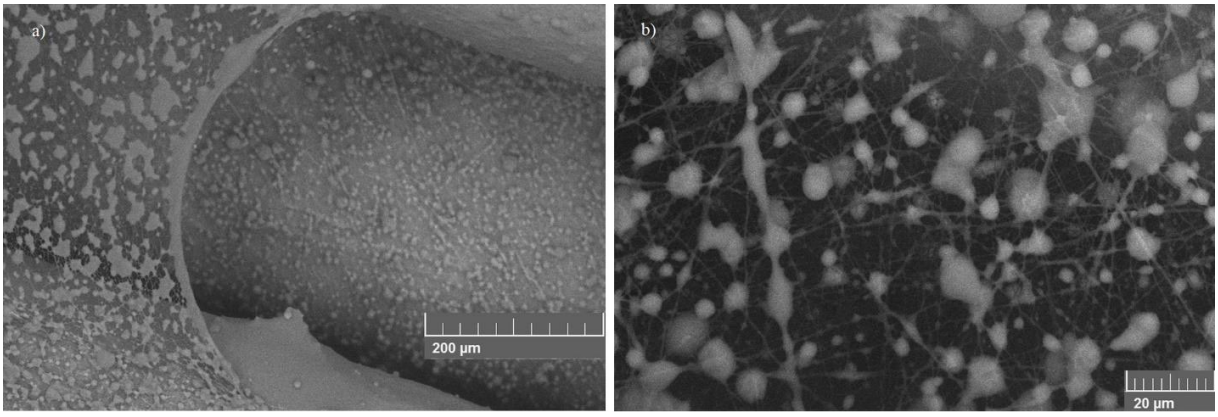

Fig. 6. Fibers and beads; (a) hybrid substrate, (b) PCL beads-on-string

Furthermore, the polymer solutions used in the electrospinning step for the hybrid scaffold manufacturing could be mixed with nanoparticles, providing the scaffolds with additional properties such as increased conductivity for supporting stem cell differentiation into neuronal cell lines. Another possibility could be the addition of biomolecules into the polymer solution in such a way that they would be released over time to the cell culture as the fibers degrade.

4. Conclusions

In this work, it was shown the concept of a machine tool for the fabrication of hybrid scaffold structures for tissue engineering applications, combining FDM, electrospinning, and micromilling capabilities. The hybrid biocompatible and biodegradable fabricated scaffolds could be used as a 3D supporting structure for cell cultures. With this machine

tool different geometries for the FDM printed structure can be explored. Multi-material, multi-scale manufacturing is achievable utilizing the described manufacturing approach.

References

[1] Lu, H., Feng, Z., Gu, Z., & Liu, C. (2009). Growth of outgrowth endothelial cells on aligned PLLA nanofibrous scaffolds. *Journal of Materials Science. Materials in Medicine*, *20*(9), 1937–44.

[2] Shin, Y. M., Park, J.-S., Jeong, S. I., An, S.-J., Gwon, H.-J., Lim, Y.-M., Kim, C.-Y. (2014). Promotion of human mesenchymal stem cell differentiation on bioresorbable polycaprolactone/biphasic calcium phosphate composite scaffolds for bone tissue engineering. *Biotechnology and Bioprocess Engineering*, *19*(2), 341–349.

[3] Hoffman-Kim, D., Mitchel, J. a, & Bellamkonda, R. V. (2010). Topography, cell response, and nerve regeneration. *Annual Review of Biomedical Engineering*, *12*, 203–31.

[4] Von Der Mark, K., Park, J., Bauer, S., & Schmuki, P. (2010). Nanoscale engineering of biomimetic surfaces: Cues from the extracellular matrix. *Cell and Tissue Research*, *339*(1), 131–153.

[5] Gupta, K. C., Haider, A., Choi, Y., & Kang, I. (2014). Nanofibrous scaffolds in biomedical applications. *Biomaterials Research*, *18*(1), 5.

[6] Wang, C., & Wang, M. (2014). Electrospun multifunctional tissue engineering scaffolds. *Frontiers of Materials Science*, *8*(1), 3–19.

[7] Ashammakhi, N., Ndreu, a., Yang, Y., Ylikauppila, H., & Nikkola, L. (2012). Nanofiber-based scaffolds for tissue engineering. *European Journal of Plastic Surgery*, *35*(2), 135–149.

[8] Schicker, M., Seitz, H., Drosse, I., Seitz, S., & Mutschler, W. (2006). Biomaterials as scaffold for bone tissue engineering. *European Journal of Trauma*, *32*(2), 114–124.

[9] Karande, T. S., Ong, J. L., & Agrawal, C. M. (2004). Diffusion in musculoskeletal tissue engineering scaffolds: design issues related to porosity, permeability, architecture, and nutrient mixing. *Annals of Biomedical Engineering*, *32*(12), 1728–1743.

[10] Lee, H., & Kim, G. (2014). Enhanced cellular activities of polycaprolactone/alginate-based cell-laden hierarchical scaffolds for hard tissue engineering applications. *Journal of Colloid and Interface Science*, *430*, 315–325.